

---

# Edge-augmented Graph Transformers: Global Self-attention is Enough for Graphs

---

**Md Shamim Hussain**

Department of Computer Science  
Rensselaer Polytechnic Institute  
110 8th St.  
Troy/NY, USA  
hussam4@rpi.edu

**Mohammed J. Zaki**

Department of Computer Science  
Rensselaer Polytechnic Institute  
110 8th St.  
Troy/NY, USA  
zaki@cs.rpi.edu

**Dharmashankar Subramanian**

IBM Research  
dharmash@us.ibm.com

## Abstract

Transformer neural networks have achieved state-of-the-art results for unstructured data such as text and images but their adoption for graph-structured data has been limited. This is partly due to the difficulty in incorporating complex structural information in the basic transformer framework. We propose a simple yet powerful extension to the transformer – residual edge channels. The resultant framework, which we call Edge-augmented Graph Transformer (EGT), can directly accept, process and output structural information as well as node information. This simple addition allows us to use global self-attention, the key element of transformers, directly for graphs and comes with the benefit of long-range interaction among nodes. Moreover, the edge channels allow the structural information to evolve from layer to layer, and prediction tasks on edges can be derived directly from these channels. In addition to that, we introduce positional encodings based on Singular Value Decomposition which can improve the performance of EGT. Our framework, which relies on global node feature aggregation, achieves better performance compared to Graph Convolutional Networks (GCN), which rely on local feature aggregation within a neighborhood. We verify the performance of EGT in a supervised learning setting on a wide range of experiments on benchmark datasets. Our findings indicate that convolutional aggregation is not an essential inductive bias for graphs and global self-attention can serve as a flexible and adaptive alternative to graph convolution.

## 1 Introduction

Graph-structured data are ubiquitous in different areas ranging from communication networks, molecular structures, citation networks, knowledge bases and social networks. A graph consists of a set of entities called nodes and the pairwise interactions among them called edges. Edges in a graph bear the structural information about the interconnectivity of the nodes. An edge can be formed arbitrarily between any pair of nodes in the graph and can bear additional information regarding the nature of connectivity, including directionality and weight. Due to the flexibility of this structural information in graphs, they are powerful tools for the compact and intuitive representation of data originating from a very wide range of sources. Graphs have more expressive power in terms of structural representation than more strictly arranged data such as sequential and time-series data (e.g.,

text, audio), grid-like data (e.g., images) and spatio-temporal data (e.g., video), especially because a graph can encode spatial and temporal information within its nodes and edges. However, this flexibility comes at the cost of added complexities in processing and learning from graph-structured data.

In the last decade, deep convolutional and recurrent neural networks have achieved unprecedented success in learning from unstructured data such as text and images. Graph Neural Networks (GNN) attempt to translate this success for graph-structured data. Following the success of deep learning in the fields of computer vision and natural language processing, there has been a renewed interest in Graph Neural Networks. The most commonly used GNNs follow a convolutional pattern whereby each node in the graph updates its state based on that of its neighbors, in each layer.

Apart from deep convolutional and recurrent neural networks, recently self-attention based transformer neural networks [1] have achieved great success in natural language processing tasks such as language understanding, machine translation and question answering. Transformers were originally conceived for sequential data, more specifically textual data. Later they were applied to other types of unstructured data, like images [2]. Transformers have achieved very good results on unstructured data in different domains such as text, audio and images and in different tasks, often establishing a new state of the art. However, transformers differ from previously ubiquitous neural network architectures, namely convolutional and recurrent neural networks in a very important way. The internal arrangement of the data, i.e., the sequential or grid-like pattern of positions does not directly dictate how it is processed by a transformer, rather, the positional information is treated as an input to the network in the form of positional encodings. Information is propagated among different positions via the global self-attention mechanism only, which is agnostic to the internal arrangement of the data. Due to this property of global self-attention, distant points in the data can interact with each other as efficiently as nearby points. Also, very little modification (only in terms of positional encodings) is required when we move from sequential to grid-like data such as images. However, the highly arbitrary nature of structure in graphs makes it is very difficult to represent the position of each node only in terms of positional encodings. Methods like Graph-BERT [3] need to employ multiple types of relative positional encodings and skip connections to efficiently incorporate the structural information within the node embeddings since the transformer architecture does not directly take structural information as an input. However, this method is not powerful enough to be generalizable to graphs of arbitrary complexities in terms of the interconnectivity of nodes. Also, it is not clear how edge features could be incorporated in such an architecture.

We introduce a new addition to the transformer, namely residual edge channels, which can facilitate both the input and the processing of structural information while only using global self-attention for propagating information among nodes. This is a simple yet powerful extension to the transformer framework in that it allows the transformer network to directly process graph-structured data. This addition is very general in the sense that, it facilitates the input of structural information of arbitrary form, including edge features, and can handle different variants of graphs such as directed and weighted graphs in a uniform manner. Additionally, we introduce a form of generalized positional encoding for all variants of graphs (including directed and weighted) based on Singular Value Decomposition of the adjacency matrix. Our framework can match and often exceed the results of widely used Graph Convolutional Networks on datasets of moderate sizes, in supervised benchmarking tasks while maintaining a similar number of parameters. But, our architecture deviates significantly from graph convolutional networks in that it does not incorporate the structural information as an inductive bias by following a strict convolutional pattern. Instead, we rely on the transformer to learn how best to use the structural information, rather than constraining it to a given input structure. Additionally, the structural information can evolve over layers and the network can potentially form new structures. Any prediction on the structure of the graph such as link prediction and edge classification can be done directly from the edge channels. However, these channels add to the already existing quadratic computational and memory complexities of the global self-attention mechanism, with respect to the number of nodes, which restricts us to medium-sized graphs.

Additionally, we introduce a new generalized positional encoding for our architecture. Since structural information is fed through the edge channels, the inclusion of positional encodings is optional for some tasks. However, positional encodings can potentially improve the performance of the network by including denoised global positional information within the nodes. Also, these encodings can assign specific roles to each node and break the symmetry in predicting edge targets (e.g., link prediction and edge classification). The proposed encoding can be thought of as a generalization of

the Laplacian eigenvectors proposed by Dwivedi et al. [4] for adjacency matrix and can be applied to directed and weighted graphs alongside undirected ones.

Our experimental results indicate that given enough data and with the proposed edge channels, the model can utilize global-self attention to learn the best aggregation pattern for the task at hand. Thus, following a fixed convolutional aggregation pattern whereby each node is limited to aggregating its closest neighbors (based on adjacency, distance, intimacy, etc.) is not an essential inductive bias. Similar findings have been reported for unstructured data such as images [5, 6]. Some recent works have reported global self-attention as a means for better generalization or performance by improving expressivity of graph convolution [7, 8]. But to our knowledge, we are the first to propose global self-attention as a direct replacement for graph convolution.

## 1.1 Related Work

There have been several attempts at adopting the self-attention mechanism for graph-structured data. Methods like Graph Attention Networks (GAT) [9] and Graph Transformer (GT) [10] constrain the self-attention mechanism to local neighborhoods of each node only. These architectures improve upon the basic Graph Convolutional Network (GCN) [11], GraphSAGE [12] and Graph Isomorphism Networks [13] by replacing the simplistic aggregation process (such as sum or mean) with local self-attention which preserves the permutation invariance among neighboring nodes while also being more expressive and adaptive. These models follow the aggregation pattern of graph convolutional networks. The convolutional pattern serves as an inductive bias to guide the update process of node states. Each convolutional layer can be thought of as a message-passing stage among neighboring nodes. The same pattern is followed within all convolutional layers, and the receptive field of each node increases by one hop with every layer of convolution.

Several works have attempted to adopt the global self-attention mechanism for graphs as well. Graph-BERT [3] uses a modified transformer framework on a sampled linkless subgraph (i.e., only node representations are processed) around a target node. Since the nodes don't inherently bear information about their interconnectivity, Graph-BERT uses several types of relative positional encodings to embed the information about the edges within a subgraph. Graph Transformer [14] directly adopts the global self-attention and encoder-decoder attention mechanism of transformers. The existing edges in the graph are incorporated by taking a weighted average of learned edges (by the attention mechanism) and existing edges. Universal Graph Transformer Self-attention Network (U2GNN) [15] uses self-attention along with a recurrent mechanism. It primarily uses a local self-attention mechanism as an aggregation function with multi-layered perceptrons as transition functions. In a later modification to the architecture, they use global self-attention (like the original transformer architecture) with convolutional transition functions. Global self-attention based aggregation has a distinctive benefit over local self-attention and convolutional aggregation in that the receptive field of each layer spans the whole graph. Thus, this mechanism can potentially capture global features within a single layer. Apart from being used as an aggregation mechanism for node features, attention has also been used to form metapaths in heterogeneous graphs [16, 17].

Our work focuses on adopting the transformer neural network with its global self-attention mechanism for graphs. Some of the above-mentioned works can be thought of as special cases of our proposed architecture. The Graph Transformer proposed by Dwivedi et al. [10] can be derived from EGT by restricting the attention mechanism and the edge channels to immediate neighbors of each node. The authors proposed that maintaining such a constrained aggregation pattern is an essential inductive bias for graphs, but our work establishes that such a sparse aggregation pattern is only potentially advantageous from a computational perspective. In general global attention can outperform local attention based aggregation when enough data is available. The Graph Transformer proposed by Li et al. [14] can be thought of as EGT with simplified edge augmentation, i.e., existing edges are directly used to loosely guide the aggregation process towards the neighbors of each node.

Positional encodings have been used for GNNs to embed global positional information within individual nodes. Additionally, they can serve to distinguish isomorphic nodes and edges in a graph [18, 19]. Murphy et al. [18] use one-hot vectors corresponding to node indices. Graph-BERT [3] uses three types of positional encodings – Weisfeiler Lehman based absolute positional encodings, the intimacy based positional encodings and the hop based positional encodings. Among these, the last two encoding schemes are relative in nature and are only relevant when performing prediction tasks on a node of interest within a sampled subgraph. Dwivedi et al. [4] proposed to use the  $k$  smallest

non-trivial eigenvectors of the Laplacian matrix of the graph as positional encodings. However, since the Laplacian eigenvectors can be complex-valued for directed graphs, this method is more relevant for undirected graphs which have symmetric Laplacian matrices. Our method can be thought of as a generalization over the eigenvectors-based positional encoding for directed graphs.

## 2 Edge-augmented Graph Transformer Architecture

We now introduce the proposed network architecture, which is an extension upon the original transformer architecture by Vaswani et al. [1]. The transformer architecture treats the input embeddings as a multiset, which is ideal for processing node embeddings in a graph. Thus, we call the residual channels present in the original transformer architecture *node channels*. These channels have the same dimensionality as the number of nodes in the input graph. Our contribution to the transformer architecture is the *edge channels*, which have the dimensionality of the number of possible edges, which scales quadratically with the number of nodes. The edge channels cooperate with the node channels during the multi-head attention based aggregation process to form the logits of the softmax attention matrices. Optionally, we can perform gated aggregation by adding sigmoid gates derived from the edge channels. The edge channels in turn are updated from the logits of the attention matrix. Thus, information can flow between both channels at each layer.

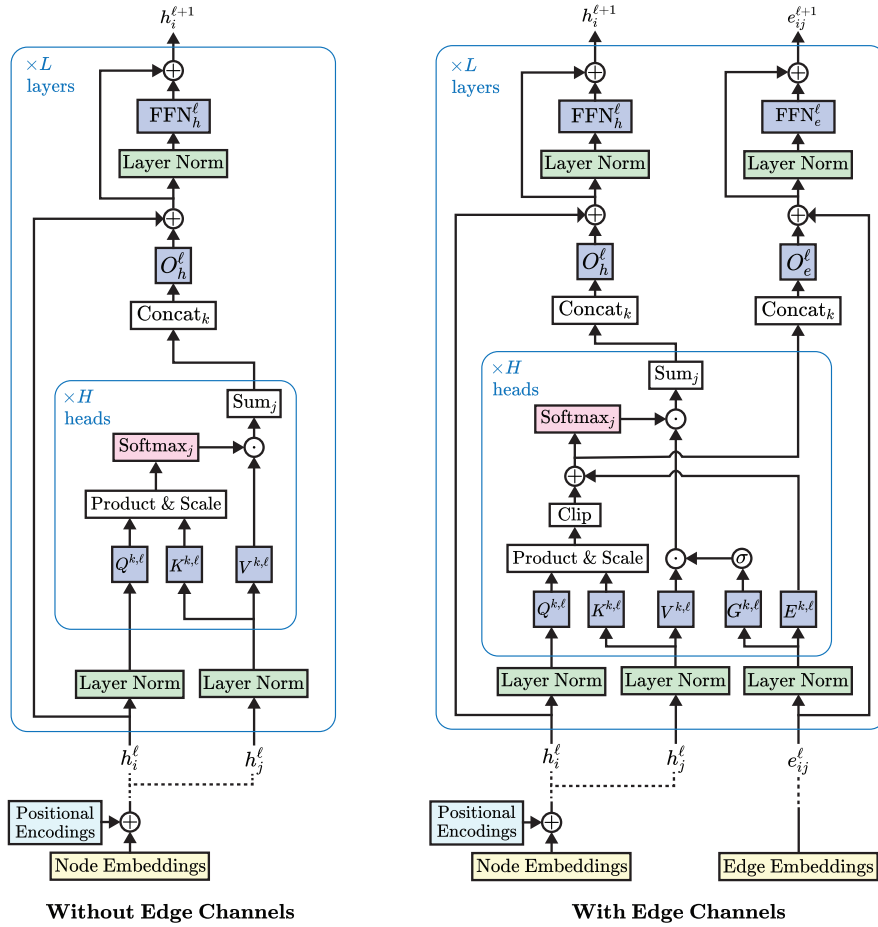


Figure 1: The basic transformer architecture with only node channels (left) and the transformer architecture augmented with edge channels (right)

## 2.1 Problem Formulation

A graph  $\mathcal{G} = (\mathcal{V}, \mathcal{E})$  is a set of nodes or vertices  $\mathcal{V}$  and a set of edges between these nodes  $\mathcal{E} \subseteq \mathcal{V} \times \mathcal{V}$ . In the case of undirected graphs,  $\mathcal{E}$  is a set of unordered pairs of vertices, whereas in the case of directed graphs it consists of ordered pair of vertices. A node may be connected to itself, and this is known as a self-loop. In the case of weighted graphs, there is a non-negative weight associated with each edge in  $\mathcal{E}$  signifying the level of interaction between the nodes connected by that edge. The interconnectivity of the nodes is signified by the edges. Thus, the edges define the structure of the graph. If there are  $|\mathcal{V}| = N$  nodes in the graph, potentially  $N^2$  edges may exist between those nodes (if we allow directed edges and self-loops), and the structure of the graph can be represented by a structural matrix of dimensionality  $N \times N$ . The simplest of these structural matrices is the adjacency matrix which represents the 1-hop connectivity between two nodes.

$$\mathbf{A} = \{a_{ij}\} \in \mathbb{R}^{N \times N} \quad (1)$$

$$a_{ij} = \begin{cases} 1 & \text{if there exists an edge from node } i \text{ to } j \\ 0 & \text{otherwise} \end{cases} \quad (2)$$

In the case of an undirected graph,  $\mathbf{A}$  is symmetric. In the case of a weighted graph,  $a_{ij}$  can take a continuous value rather than 0 or 1. Self-loops can be represented by setting the diagonal elements  $a_{ii} = 1$ . Thus, the structure of all these different variants of graphs can be expressed by the adjacency matrix. The rows of the adjacency matrix can be normalized so that they sum up to 1, this is called the normalized adjacency matrix. There are other matrices with dimensionality  $N \times N$  which can completely or partially define the structure of a graph (e.g., the Laplacian Matrix). We will be calling them graph structural matrices in general.

Additionally, a graph may have node features and edge features associated with its nodes and edges, respectively. We will denote the node features associated with node  $i$  as  $\alpha_i$  and the edge features for the edge  $(i, j)$  as  $\beta_{ij}$ .

## 2.2 Transformers and Graphs

The transformer neural network [1] (Fig. 1 left) transforms a set of embeddings  $\{h_1^0, h_2^0, \dots, h_N^0\}$  into a set of output embeddings  $\{(h_1^L)_{final}, (h_2^L)_{final}, \dots, (h_N^L)_{final}\}$  where  $N$  is the number of positions which, in the case of a graph, is the number of nodes and  $L$  is the number of layers. All embeddings are vectors of the same dimensionality, i.e.,  $h_i^\ell \in \mathbb{R}^{d_h}$ . Each layer consists of two sublayers. The first one is a multi-head self-attention sublayer which aggregates the values of all positions via a query and key based scaled dot product attention weighting process. The keys, queries and values are formed by learned linear projections. This aggregation process is done multiple times, i.e., for each of the attention heads, and then the outputs are merged through another linear projection. Mathematically the aggregation process at the  $\ell$ 'th layer can be expressed as:

$$(\hat{h}_i^\ell)_{mha} = \mathbf{O}_h^\ell \parallel \sum_{k=1}^H \sum_{j=1}^N w_{ij}^{k,\ell} \mathbf{V}^{k,\ell} \hat{h}_j^\ell \quad (3)$$

$$\text{Where, } w_{ij}^{k,\ell} = \text{softmax}_j \left( \frac{(\mathbf{Q}^{k,\ell} \hat{h}_i^\ell)^T (\mathbf{K}^{k,\ell} \hat{h}_j^\ell)}{\sqrt{d_k}} \right) \quad (4)$$

Here,  $\hat{h}_i^\ell$  and  $(\hat{h}_i^\ell)_{mha}$  for  $i \in \{1, 2, \dots, N\}$  are the input and output features of the multihead attention module, respectively.  $H$  is the number of attention heads.  $\mathbf{Q}^{k,\ell}, \mathbf{K}^{k,\ell}, \mathbf{V}^{k,\ell} \in \mathbb{R}^{d_k \times d_h}$  are learned projection matrices for queries, keys and values respectively for the  $k$ 'th head.  $\text{softmax}_j$  denotes the  $j$ 'th component of the softmax over all  $j \in \{1, 2, \dots, N\}$ .  $\parallel$  denotes concatenation of the outputs of the attention heads.  $\mathbf{O}_h^\ell \in \mathbb{R}^{d_h \times d_k}$  is the learned output projection matrix, where  $d_k$  is the dimensionality of the query, key and value vectors. The aggregation process, i.e., the weighted sum can be performed efficiently by matrix multiplication with

$$\text{Attention}(\mathbf{Q}_h^{k,\ell}, \mathbf{K}_h^{k,\ell}, \mathbf{V}_h^{k,\ell}) = \text{softmax} \left( \frac{\mathbf{Q}_h^{k,\ell} (\mathbf{K}_h^{k,\ell})^T}{\sqrt{d_k}} \right) \mathbf{V}_h^{k,\ell} = \tilde{\mathbf{A}}^{k,\ell} \mathbf{V}_h^{k,\ell} \quad (5)$$

where  $\mathbf{Q}_h^{k,\ell}, \mathbf{K}_h^{k,\ell}, \mathbf{V}_h^{k,\ell} \in \mathbb{R}^{N \times d_k}$  denote concatenation of  $\mathbf{Q}^{k,\ell} \hat{h}_i^\ell, \mathbf{K}^{k,\ell} \hat{h}_i^\ell, \mathbf{V}^{k,\ell} \hat{h}_i^\ell$ , respectively, for  $i \in \{1, 2, \dots, N\}$ .  $\tilde{\mathbf{A}}^{k,\ell} \in \mathbb{R}^{N \times N}$  are the attention matrices. We can compare each of the attention

matrices with a normalized adjacency matrix of a weighted complete graph. They dictate how the node features in a graph are aggregated, similar to GCN [11]. However, unlike the input graph this graph is dynamically formed by the attention mechanism for each attention head.

To facilitate training deep networks with gradient descent it is customary to use some form of normalization [20, 21] and residual connections [22]. These features are adopted by the transformer architecture as well. The original architecture by Vaswani et al. [1] used layer normalization [21] after the residual connections (Post-Norm), however later it was observed that it is easier to train the architecture if normalization is done immediately before the weighted sublayers (Pre-Norm) [23]. In the Pre-Norm setting, the attention sublayer takes the form :

$$\hat{h}_i^\ell = \text{LayerNorm}(h_i^{\ell-1}) \quad (6)$$

$$\hat{h}_i^\ell = h_i^{\ell-1} + \mathbf{O}_h^\ell \parallel \sum_{k=1}^H \sum_{j=1}^N \text{softmax}_j \left( \frac{(\mathbf{Q}^{k,\ell} \hat{h}_i^\ell)^T (\mathbf{K}^{k,\ell} \hat{h}_j^\ell)}{\sqrt{d_k}} \right) \mathbf{V}^{k,\ell} \hat{h}_i^\ell \quad (7)$$

The attention sublayer is followed by a feed-forward sublayer which applies a pointwise non-linear transformation on the embeddings. Usually, this is achieved by two consecutive pointwise fully connected linear layers with a non-linearity such as ELU [24] in between.

$$\hat{\hat{h}}_i^\ell = \text{LayerNorm}(\hat{h}_i^\ell) \quad (8)$$

$$h_i^\ell = \hat{\hat{h}}_i^\ell + \mathbf{W}_{h,2}^\ell \text{ELU}(\mathbf{W}_{h,1}^\ell \hat{\hat{h}}_i^\ell + b_{h,1}^\ell) + b_{h,2}^\ell \quad (9)$$

The Pre-Norm transformer architecture also ends with a layer normalization over the final embeddings.

$$(h_i^L)_{\text{final}} = \text{LayerNorm}(h_i^L) \quad (10)$$

### 2.3 Edge Channels

The basic transformer architecture mentioned in the previous section is capable of processing node embeddings in a graph by updating each node's embedding based on the weighted aggregation of all node features. This is a direct application of global self-attention for graphs. Also, we mentioned that this operation is equivalent to graph convolution in multiple complete weighted graphs which are dynamically formed by the attention mechanism. However, we do not have a direct way to incorporate the input structure (existing edges) while forming these weighted graphs, i.e., the attention matrices. Also, these dynamic graphs are collapsed immediately after the aggregation process is done. The node embeddings themselves have to bear the necessary information to represent any new structural features that we may want the network to predict, for example, new edges or even the labels of the existing edges. To remedy these problems we introduce new residual channels which bear the responsibility of input and processing of pairwise structural features, i.e., information regarding both existing and possible edges. The Edge-augmented Graph Transformer is shown in Fig. 1 on the right.

Similar to node channels, the edge channels start with an embedding for each pair of nodes. Thus, there are  $N \times N$  input embeddings  $e_{11}^0, e_{12}^0, \dots, e_{1N}^0, e_{21}^0, \dots, e_{NN}^0$ . These embeddings have dimensionality  $e_{ij}^l \in \mathbb{R}^{d_e}$ . The input embeddings are formed by learnable transformations of the graph structural matrices and the edge features. For the non-existing edges, either a masking token (for discrete values) or a masking value (for continuous input) is used as input. These embeddings are updated by the EGT in each layer and finally it produces a set of output embeddings  $(e_{11}^L)_{\text{final}}, (e_{12}^L)_{\text{final}}, \dots, (e_{1N}^L)_{\text{final}}, (e_{21}^L)_{\text{final}}, \dots, (e_{NN}^L)_{\text{final}}$ . From these output embeddings, we can perform structural predictions such as edge labeling and link prediction.

In our modified architecture the edge channels participate in the self-attention sublayer to dictate how the node features are aggregated. This is done by adding an additional term to the input of the softmax function which is derived from the edge channels. Also, we clip the scaled dot product to a limited range  $[\mu, \nu]$  which leads to better numerical stability. In our experiments we used  $\mu = -5$  and  $\nu = +5$ , i.e., a range of  $[-5, +5]$ .

$$w_{ij}^{k,\ell} = \text{softmax}_j \left( \hat{w}_{ij}^{k,\ell} \right) \quad (11)$$

$$\text{Where, } \hat{w}_{ij}^{k,\ell} = \max \left( \mu, \min \left( \nu, \frac{(\mathbf{Q}^{k,\ell} \hat{h}_i^\ell)^T (\mathbf{K}^{k,\ell} \hat{h}_j^\ell)}{\sqrt{d_k}} \right) \right) + E^{k,\ell} e_{ij}^\ell \quad (12)$$

We denote the input to the softmax function as  $\hat{w}_{ij}^{k,\ell}$ . Adding a gating mechanism to the aggregation process slightly improves final results. In the gated variant, weights are calculated as

$$w_{ij}^{k,\ell} = \text{softmax}_j \left( \hat{w}_{ij}^{k,\ell} \right) \sigma(G^{k,\ell} \hat{e}_{ij}^\ell) \quad (13)$$

Where,  $\sigma(\cdot)$  is the logistic sigmoid activation function.  $E^{k,\ell}, G^{k,\ell} \in \mathbb{R}^{1 \times d_e}$  are learned projection matrices. Additionally, the edge embeddings themselves are modified based on the inputs to the softmax function. We use normalization and residual connections for edge channels similar to node channels. The modified updates for the self-attention sublayer are given as

$$\hat{h}_i^\ell = \text{LayerNorm}(h_i^{\ell-1}) \quad (14)$$

$$\hat{e}_{ij}^\ell = \text{LayerNorm}(e_{ij}^{\ell-1}) \quad (15)$$

$$\hat{h}_i^\ell = h_i^{\ell-1} + \mathbf{O}_h^\ell \parallel \sum_{k=1}^H \sum_{j=1}^N w_{ij}^{k,\ell} \mathbf{V}^{k,\ell} \hat{h}_i^\ell \quad (16)$$

$$\hat{e}_{ij}^\ell = e_{ij}^{\ell-1} + \mathbf{O}_e^\ell \parallel \hat{w}_{ij}^{k,\ell} \quad (17)$$

Here,  $\mathbf{O}_e^\ell \in \mathbb{R}^{d_e \times H}$  is a learned projection matrix. Similar to node channels, the edge channels are also updated in a pointwise manner by feed-forward sublayers.

$$\hat{\hat{e}}_{ij}^\ell = \text{LayerNorm}(\hat{e}_{ij}^\ell) \quad (18)$$

$$e_{ij}^\ell = \hat{\hat{e}}_{ij}^\ell + \mathbf{W}_{e,2}^\ell \text{ELU}(\mathbf{W}_{e,1}^\ell \hat{\hat{e}}_{ij}^\ell + b_{e,1}^\ell) + b_{e,2}^\ell \quad (19)$$

Following the Pre-Norm architecture, the edge channels also end with a layer normalization over the final edge embeddings.

$$(e_{ij}^D)_{final} = \text{LayerNorm}(e_{ij}^D) \quad (20)$$

## 2.4 SVD-based Positional Encodings

The transformer encoder is permutation equivariant. In other words, it treats its input embeddings as a (multi) set. To distinguish different positions and to encode the distances of different positions, the information about positions needs to be encoded within the embeddings themselves. For sequential data such as text, it is customary to use sinusoidal positional encodings introduced by Vaswani et al. [1]. However, the arbitrary nature of structure in graphs makes it difficult to devise a consistent positional encoding scheme. Since the basic transformer architecture does not directly take structural input, Graph-BERT [3] has to encode all structural information as positional encodings in its linkless subgraph method. Our architecture directly takes structure as input and thus does not face this difficulty. On the other hand, convolutional architectures like GCN [11] and GAT [9] use the structural information as an inductive bias during the aggregation process. You et al. [25] mention that for convolutional networks it is useful to encode global position in the form of positional encodings because the receptive fields of these networks are limited and may not span the whole graph. Our architecture does not face this problem either because of the use of global self-attention which spans the whole graph. Due to these features of our proposed architecture, we predict that positional encodings are optional for most tasks. However, for some tasks, we noticed an improvement while using positional encodings. We believe this is due to two reasons. First, positional encodings can serve as a source of denoised global positional information within a graph, robust to small perturbations. This is inspired by the matrix factorization based node embedding methods for graphs [26]. Second, positional encodings can help distinguish isomorphic nodes which may be necessary to form appropriate edge representations [27].

We propose a form of positional encoding based on precalculated Singular Value Decomposition of the graph structural matrices. We use the largest  $r$  singular values and corresponding left and right singular vectors to form our positional encodings. Primarily, we use the adjacency matrix  $\mathbf{A}$  (with self-loops) as the graph structural matrix, but this method can be generalized to any graph structural

matrix since the SVD of any real matrix produces real singular values and singular vectors.

$$\mathbf{A} = \{a_{ij}\} \stackrel{\text{SVD}}{=} \mathbf{U}\mathbf{\Sigma}\mathbf{V}^T \approx \hat{\mathbf{U}}\hat{\mathbf{V}}^T \quad (21)$$

$$\text{Where, } \hat{\mathbf{U}} = \mathbf{U}_{1:N, 1:r} \mathbf{\Sigma}_{1:r, 1:r}^{\frac{1}{2}} \quad (22)$$

$$\text{And, } \hat{\mathbf{V}} = \mathbf{V}_{1:N, 1:r} \mathbf{\Sigma}_{1:r, 1:r}^{\frac{1}{2}} \quad (23)$$

$$\text{Finally, } \hat{\mathbf{\Gamma}} = \hat{\mathbf{U}} \parallel \hat{\mathbf{V}} \quad (24)$$

Where  $\mathbf{U}$  and  $\mathbf{V}$  matrices contain the left and the right singular vectors as columns, respectively, and the diagonal  $\mathbf{\Sigma}$  matrix contains the singular values.  $\parallel$  denotes concatenation along columns. From (21) we see that the dot product between  $i$ 'th row of  $\hat{\mathbf{U}}$  and  $j$ 'th row of  $\hat{\mathbf{V}}$  can approximate  $a_{ij}$  which denotes whether there is an edge between nodes  $i$  and  $j$ . Thus, the rows of  $\hat{\mathbf{\Gamma}}$ , namely  $\hat{\gamma}_1, \hat{\gamma}_2, \dots, \hat{\gamma}_N$ , each with dimensionality  $\hat{\gamma}_i \in \mathbb{R}^{2r}$ , bear denoised information about the edges and can be used as positional encodings. Note that this form of representation based on dot product is consistent with the scaled dot product attention used in the transformer framework.

Since the signs of corresponding pairs of left and right singular vectors can be arbitrarily flipped, we can randomly flip the signs of  $\hat{\gamma}_i$  during training. This can be thought of as a form of data augmentation that makes the model more robust to the input positional encodings that can be especially important for smaller datasets on which the model tends to overfit. However, as we will show in a later section, this form of augmentation may not be necessary for a larger dataset.

Instead of directly adding  $\hat{\gamma}_i$  to the input embeddings of the node  $i$ , we add a projection  $\gamma_i = \mathbf{W}_{enc}\hat{\gamma}_i$ , where  $\mathbf{W}_{enc} \in \mathbb{R}^{d_h \times 2r}$  is a learned projection matrix. This heuristically leads to better results. SVD is performed before training as a data preprocessing step and thus does not affect training time.

Note that if we apply SVD on a symmetric positive semi-definite matrix like the Laplacian matrix of an undirected graph, it is equivalent to Eigenvalue Decomposition (EVD). Thus, our method can be thought of as a generalization of the Laplacian eigenvector-based positional encodings proposed by Dwivedi et al. [4] for directed graphs and any graph structural matrix (in our case the adjacency matrix).

## 2.5 Embedding and Task-specific Layers

As mentioned before we have  $N$  node embeddings of dimensionality  $d_h$  and also  $N \times N$  edge (i.e., pairwise) embeddings of dimensionality  $d_e$ . We will call  $d_h$  and  $d_e$  the width of the node and edge channels, respectively. The node embeddings are formed by performing learnable linear transformation (for continuous vector values) or vector embedding (for categorical/discrete values) of node features  $\alpha_1, \alpha_2, \alpha_3, \dots, \alpha_N$  to form embeddings of dimensionality  $d_h$ . In the case of multiple sets of features, their corresponding embeddings can be added together. In case positional encodings are used, they are also transformed by a learnable transformation as mentioned in the previous section to obtain  $\gamma_i$ , and added to the node embeddings before they are fed through the node channels (Fig. 1). In the absence of edge features, the edge embeddings are formed by a learnable linear transformation or vector embedding of the members of the graph structural matrix. We use the unnormalized graph adjacency matrix with self-loops  $\mathbf{A} = \{a_{ij}\}$  where  $a_{ij} \in \{0, 1\}$ , so we use vector embeddings of these two discrete values. If edge features are present, they are transformed by learnable transformations or vector embeddings, and  $e_{ij}$  is formed by adding together embeddings from structural matrices ( $a_{ij}$ ) and edge features ( $\beta_{ij}$ ). Finally, these embeddings are fed through the edge channels. Masked attention can be used to process mini-batches containing graphs of different numbers of nodes. This allows us to use highly parallelized tensor operations on the GPU while training the network with minibatch gradient descent and also during simultaneous prediction on multiple input graphs.

Once the embeddings are transformed by the EGT, they are passed through a few additional layers depending on the task to be performed. In the case of node classification/regression, we apply two pointwise linear layers on the node embeddings with ELU activation and output dimensions of  $\frac{d_h}{2}$  and  $\frac{d_h}{4}$ , correspondingly. Finally, a linear layer with appropriate output dimensions is added for classification (softmax activation) or regression (linear activation). In the case of graph classification/regression, all the output node embeddings are averaged (i.e., global average pooling) to form a graph-level embedding, on which final linear layers are applied. In the case of edge classifica-



tion/regression, we use the edge embeddings which are fed to the final linear layers in a pointwise manner to produce edge labels or to predict new links.

### 3 Experimental Methodology

We primarily evaluate the performance of our proposed architecture in a supervised and inductive setting. We focus on a diverse set of supervised learning tasks, namely, node classification, graph classification and regression, and edge classification.

#### 3.1 Datasets Description

To evaluate our architecture we use the benchmarking datasets proposed by Dwivedi et al. [4]. We chose these datasets over more commonly used smaller datasets (e.g., Cora [28], Citeseer [29] and TU [30]), which are often used to evaluate other GNN architectures for several reasons. As mentioned by Dwivedi et al., these smaller datasets often cannot statistically distinguish the performance levels of different GNN architectures. We wanted to establish the performance level of our proposed architecture against other commonly used architectures for a set of very general machine learning tasks on graphs, so we found existing benchmarks for other well-known architectures useful. Also, the numbers of nodes in the input graphs in these datasets are tractable in terms of quadratic computational and memory complexities of the proposed global self-attention based architecture. Another very important reason for choosing datasets of moderate sizes is the fact that we do not directly utilize the strong inductive bias of convolutional GNNs, instead, we rely on the network to interpret how best to utilize the structural information. This flexibility (i.e., higher capacity) of our model could lead to overfitting on smaller datasets. We experiment on the following datasets.

**PATTERN** is a node classification dataset generated using the Stochastic Block Model [31] which poses the task of classifying the nodes in a graph into two communities. There are a total of 14K graphs in the dataset, each with 44-188 nodes. The nodes have discrete node features associated with them but there are no edge features.

**CLUSTER** is also a node classification dataset generated using the Stochastic Block Model. It poses the task of classifying the nodes in each graph into 6 different clusters. There are a total of 12K graphs in the dataset, each with 41-190 nodes. Discrete node features are present for each node. Edge features are absent.

**MNIST** is a graph classification dataset. It is a superpixels dataset [32] produced from the well-known MNIST dataset of handwritten digits [33]. The goal is to classify each superpixel graph into 10 different classes. Both node and edge features are present and they take continuous (vector) values. There are a total of 60K graphs, each with 40-75 nodes.

**CIFAR10** is also a superpixels graph classification dataset produced from the well-known CIFAR10 dataset of tiny natural images [34]. The given task is to classify each superpixel graph into 10 different classes. Both node and edge features are present and they take continuous (vector) values. There are a total of 45K graphs, each with 85-150 nodes.

**TSP** is an edge classification dataset based on the Traveling Salesman Problem in the 2D plane, which is a well-studied NP-hard problem. The goal is to predict whether the edges in a  $k$  nearest neighbor graph formed from the vertices in the 2D plane, belong to the solution or not. There are 12K graphs in total, each with 50-500 nodes. Both (continuous-valued) node and edge features are present.

**ZINC** [35] is a dataset of real-world molecular graphs. The goal is to predict a continuous real value (constrained solubility) from the molecular graph, i.e., this is a graph regression problem. Dwivedi et al. use a subset of 12K randomly sampled graphs, each with 9-37 nodes, for the benchmarking task from the bigger dataset. We perform our experiments on the same subset. Discrete node and edge features are present.

**ZINC-FULL** is the larger dataset of which ZINC is a subset. It consists of 220K molecular graphs, each with 6-39 nodes. Although this dataset is not one of the benchmarking datasets, we use it in the ablation study.

For more information on these datasets please refer to [4].

### 3.2 Training and Evaluation Methodology

We compare our architecture with other well-known GNN architectures while keeping the number of parameters comparable. We also keep the number of layers ( $L$ ) the same, when possible. We always used 8 attention heads, but the width of the node and edge channels ( $d_h$  and  $d_e$ , correspondingly) were varied to get the best results on the validation set. Positional encodings, when used are formed from 8 singular values, 8 left singular vectors and 8 right singular vectors (rank-8 approximation). We used the Adam optimizer [36] with initial learning rate of  $5 \times 10^{-4}$ . We used a batch size of 128 for all datasets, except TSP for which a batch size of 8 is used. We reduce the learning rate by a factor of 0.5 if the validation loss does not improve for a given number of epochs (20 for ZINC, 5 for TSP, 10 for all others). We noticed a considerable amount of overfitting on some datasets if we keep training the network indefinitely, so we keep track of the validation loss at the end of each epoch and pick the set of weights that produces the least validation loss. This is a form of early stopping, a common method of regularization for deep neural networks. (Class-balanced) cross-entropy loss is used for categorical targets and Mean Absolute Error (MAE) loss is used for the regression task on the ZINC dataset. We evaluate the architectures based on an appropriate metric (e.g., weighted accuracy for node classification, accuracy for graph classification, MAE for graph regression, F1 score for edge classification on TSP) for each dataset, as recommended by the authors. We use the same definition of weighted accuracy as Dwivedi et al., which is equal to the micro averaged recall of all classes. Each experiment (training and evaluation) was run 4 times with 4 different random seeds and the results were used to calculate the mean and standard deviations of the metric. We did not use any form of regularization except for early stopping.

### 3.3 Hardware and Software Details

Both training and evaluations were done on the NPL cluster of the AiMOS supercomputer at RPI. Each model was trained on a single node of the cluster. Each node has two 20-core 2.5 GHz Intel Xeon Gold 6248 CPUs with 768 GiB of RAM and 8 NVIDIA Tesla V100 GPUs with 32 GiB of VRAM per GPU. We used the Tensorflow 2.1 [37] numerical library with the high-level Keras framework to implement and train the models. The training was done in a distributed manner over 8 GPUs with the Multiworker Mirrored Strategy which copies the model weights to each GPU and uses efficient allreduce methods to achieve effective parallelization within each mini-batch. Training time varied from half an hour to four hours.

## 4 Experimental Results and Discussions

In this section, we will present the experimental results for our Edge-augmented Graph Transformer architecture on the benchmarking datasets and compare it against other well-established Graph Neural Networks. Also, we perform an ablation study to verify the importance of different features of our model and the proposed positional encoding scheme.

### 4.1 Results

The results are presented in Table 1. For baselines, we compared our results against the most well-known and best performing GNN models on the benchmarking datasets, namely GCN [11], GraphSage [38], GAT [9] and GatedGCN [39]. These results are acquired from Dwivedi et al. [4]. The authors found that GatedGCN consistently outperformed all other architectures in the given experimental setup. Additionally, we included results for GT [10] since it is architecturally similar to our model but uses local rather than global attention. Among these architectures, only GT and GatedGCN take edge features (when available) as input, whereas others only rely on node features. Our proposed architecture, EGT takes edge features as input when available. To observe the effect of our gating mechanism proposed in (13) we present the results for gated (EGT-G) and ungated (EGT-U) variants of our architecture. Also, to explore the effect of including positional encodings, results with (suffix -PE) and without positional encodings are presented. GT and GatedGCN use Laplacian eigenvectors based positional encodings. Our model (EGT) uses SVD-based positional encodings.

From the results in Table 1 we can see that the proposed EGT architecture performs at the same level as the best-performing existing GNN, i.e., GatedGCN on the ZINC dataset while outperforming it on

Table 1: Experimental results on 6 benchmarking datasets. We compared our results against GCN [11], GraphSage [38], GAT [9], GT [10] and GatedGCN [39]. The baseline results for existing GNNs are reported from Dwivedi et al. [4, 10]. Among these GNNs, only GT and GatedGCN take edge features as input. The -EPE suffix indicates that positional encodings based on eigenvectors of the Laplacian matrix are used. Whereas, the -SPE suffix indicates that positional encodings based on SVD of the Adjacency Matrix are used. The -A suffix indicates that the positional encodings are augmented by randomly flipping the signs of the eigenvectors/singular vectors. We experimented with two variants of our Edge-augmented Graph Transformer (EGT). The suffix -G denotes gated whereas -U denotes ungated. Results on PATTERN and CLUSTER datasets are given in terms of weighted accuracy. Best results are shown in bold; for accuracy higher is better, whereas for MAE (used for ZINC) lower is better.

Model	PATTERN						CLUSTER					
	$L$	#Param	$d_h$	$d_e$	Test Acc. $\pm$ s.d.	Train Acc. $\pm$ s.d.	$L$	#Param	$d_h$	$d_e$	Test Acc. $\pm$ s.d.	Train Acc. $\pm$ s.d.
GCN	16	500823	-	-	71.892 $\pm$ 0.334	78.409 $\pm$ 1.592	16	501687	-	-	68.498 $\pm$ 0.976	71.729 $\pm$ 2.121
GraphSage	16	502842	-	-	50.492 $\pm$ 0.001	50.487 $\pm$ 0.005	16	503350	-	-	63.844 $\pm$ 0.110	86.710 $\pm$ 0.167
GAT	16	526990	-	-	78.271 $\pm$ 0.186	90.212 $\pm$ 0.476	16	527874	-	-	70.587 $\pm$ 0.447	61.618 $\pm$ 0.536
GT	10	522742	-	-	83.949 $\pm$ 0.303	83.864 $\pm$ 0.489	10	523146	-	-	72.139 $\pm$ 0.405	85.857 $\pm$ 0.555
GT-EPE-A	10	522982	-	-	84.808 $\pm$ 0.068	86.559 $\pm$ 0.116	10	524026	-	-	73.169 $\pm$ 0.622	86.585 $\pm$ 0.905
GatedGCN	16	502223	-	-	85.568 $\pm$ 0.088	86.007 $\pm$ 0.123	16	502615	-	-	73.840 $\pm$ 0.326	87.880 $\pm$ 0.908
GatedGCN-EPE-A	16	502457	-	-	86.508 $\pm$ 0.085	86.801 $\pm$ 0.133	16	504253	-	-	76.082 $\pm$ 0.196	88.919 $\pm$ 0.720
EGT-U	16	545522	64	8	86.811 $\pm$ 0.040	86.807 $\pm$ 0.042	16	545846	64	8	76.811 $\pm$ 0.333	80.112 $\pm$ 1.088
EGT-G	16	546674	64	8	<b>86.825 <math>\pm</math> 0.032</b>	86.792 $\pm$ 0.044	16	546998	64	8	77.080 $\pm$ 0.361	80.264 $\pm$ 1.251
EGT-G-EPE-A	16	546674	64	8	<b>86.856 <math>\pm</math> 0.013</b>	86.814 $\pm$ 0.008	16	546998	64	8	76.952 $\pm$ 0.337	80.106 $\pm$ 1.085
EGT-G-SPE	16	547762	64	8	86.730 $\pm$ 0.036	86.804 $\pm$ 0.035	16	548086	64	8	<b>77.909 <math>\pm</math> 0.245</b>	80.730 $\pm$ 0.491

Model	MNIST						CIFAR10					
	$L$	#Param	$d_h$	$d_e$	Test Acc. $\pm$ s.d.	Train Acc. $\pm$ s.d.	$L$	#Param	$d_h$	$d_e$	Test Acc. $\pm$ s.d.	Train Acc. $\pm$ s.d.
GCN	4	101365	-	-	90.705 $\pm$ 0.218	97.196 $\pm$ 0.223	4	101657	-	-	55.710 $\pm$ 0.381	69.532 $\pm$ 2.121
GraphSage	4	104337	-	-	97.312 $\pm$ 0.097	100.000 $\pm$ 0.000	4	104517	-	-	65.767 $\pm$ 0.308	99.719 $\pm$ 0.167
GAT	4	110400	-	-	95.535 $\pm$ 0.205	99.994 $\pm$ 0.008	4	110704	-	-	64.223 $\pm$ 0.455	89.114 $\pm$ 0.536
GatedGCN	4	104217	-	-	97.340 $\pm$ 0.143	100.000 $\pm$ 0.000	4	104357	-	-	<b>67.312 <math>\pm</math> 0.311</b>	87.880 $\pm$ 0.908
EGT-U	4	138538	64	8	97.368 $\pm$ 0.369	99.444 $\pm$ 0.397	4	138666	64	8	61.275 $\pm$ 0.966	72.084 $\pm$ 1.832
EGT-G	4	138826	64	8	<b>97.615 <math>\pm</math> 0.050</b>	99.346 $\pm$ 0.211	4	138945	64	8	63.260 $\pm$ 0.735	71.878 $\pm$ 1.363
EGT-G-SPE-A	4	139914	64	8	97.573 $\pm$ 0.068	99.550 $\pm$ 0.079	4	140042	64	8	63.968 $\pm$ 1.252	72.774 $\pm$ 2.751

Model	TSP						ZINC					
	$L$	#Param	$d_h$	$d_e$	Test F1 $\pm$ s.d.	Train F1 $\pm$ s.d.	$L$	#Param	$d_h$	$d_e$	Test MAE $\pm$ s.d.	Train MAE $\pm$ s.d.
GCN	4	95702	-	-	0.630 $\pm$ 0.001	0.631 $\pm$ 0.001	16	505079	-	-	0.367 $\pm$ 0.011	0.128 $\pm$ 0.019
GraphSage	4	99263	-	-	0.665 $\pm$ 0.003	0.669 $\pm$ 0.003	16	505341	-	-	0.398 $\pm$ 0.002	0.081 $\pm$ 0.009
GAT	4	96182	-	-	0.671 $\pm$ 0.002	0.673 $\pm$ 0.002	16	531345	-	-	0.384 $\pm$ 0.007	0.067 $\pm$ 0.004
GT	10	588353	-	-	0.264 $\pm$ 0.008	0.048 $\pm$ 0.006	10	588939	-	-	<b>0.226 <math>\pm</math> 0.014</b>	0.059 $\pm$ 0.011
GT-EPE-A	10	588939	-	-	0.282 $\pm$ 0.015	0.074 $\pm$ 0.016	16	504309	-	-	0.282 $\pm$ 0.015	0.074 $\pm$ 0.016
GatedGCN	4	97858	-	-	0.808 $\pm$ 0.003	0.811 $\pm$ 0.003	16	505011	-	-	<b>0.214 <math>\pm</math> 0.013</b>	0.067 $\pm$ 0.019
GatedGCN-EPE-A	16	500770	-	-	0.838 $\pm$ 0.002	0.850 $\pm$ 0.001	16	505011	-	-	<b>0.214 <math>\pm</math> 0.013</b>	0.067 $\pm$ 0.019
EGT-U	16	523074	64	8	0.839 $\pm$ 0.002	0.844 $\pm$ 0.003	10	501777	64	64	0.371 $\pm$ 0.020	0.103 $\pm$ 0.036
EGT-G	4	116226	64	8	0.807 $\pm$ 0.004	0.807 $\pm$ 0.003	10	506977	64	64	0.302 $\pm$ 0.023	0.067 $\pm$ 0.017
EGT-G-EPE-A	16	524226	64	8	<b>0.845 <math>\pm</math> 0.001</b>	0.850 $\pm$ 0.002	10	506977	64	64	0.242 $\pm$ 0.010	0.072 $\pm$ 0.032
EGT-G-SPE-A	4	117314	64	8	0.810 $\pm$ 0.003	0.811 $\pm$ 0.004	10	508065	64	64	<b>0.223 <math>\pm</math> 0.007</b>	0.042 $\pm$ 0.007
	16	525314	64	8	0.844 $\pm$ 0.002	0.849 $\pm$ 0.003	16	532425	56	40	<b>0.227 <math>\pm</math> 0.007</b>	0.044 $\pm$ 0.011

datasets such as CLUSTER, TSP, MNIST and PATTERN. We highlight the results on the TSP dataset where we directly used edge embeddings, rather than node embeddings (used by other GNNs) for edge classification. However, the results on the CIFAR10 dataset are worse compared to GatedGCN. This may be due to the fact that the CIFAR10 dataset is a superpixels dataset of a diverse set of natural images, but it is quite small in terms of the number of training samples. This is evident from the fact that all models, including ours, show significant overfitting on this dataset. This makes it hard for the EGT architecture to make the best use of the structural information because we do not impose the convolutional aggregation pattern as a strict inductive bias. GNNs like GatedGCN are at an advantage in this situation because of the incorporation of the convolutional inductive bias, which reduces overfitting. However, we posit that the EGT would reach or exceed the performance level of GatedGCN if more training data were present.

Apart from our architecture, GAT and GT also incorporate the attention mechanism in their aggregation process. However, unlike our architecture, they use local attention rather than global attention and follow a convolutional pattern by only aggregating within neighboring nodes. We see that our architecture, which uses only global self-attention in the aggregation process, outperforms these local

attention based models. This indicates that convolutional aggregation is not an essential inductive bias, and given enough data global attention can learn to make the best use of structural information. This in turn leads to better results.

We see that the addition of the gating mechanism consistently improves the performance of our architecture on all datasets, albeit at the cost of a slight increase in the number of parameters. However, we see that the inclusion of positional encodings does not always improve the results significantly. This is consistent with our proposal that positional encodings are optional for most tasks. However, on the ZINC dataset, we see a significant improvement in the result when positional encodings are incorporated. This is also true for GT and GatedGCN which use Laplacian eigenvectors as positional encodings. Thus, for some tasks, positional encodings can still be considered useful.

We found that our SVD based positional encodings performed at the same level or better than the more specialized Laplacian eigenvectors based positional encodings. Note that, Laplacian eigenvectors based positional encodings only apply to datasets containing undirected graphs, e.g., PATTERN, CLUSTER and ZINC. From the results on the validation set, we noticed that the augmentation of SVD based positional encodings by flipping the signs of the singular vectors is unnecessary for PATTERN and CLUSTER datasets. So, results for the un-augmented case are presented. We discuss more about the necessity for augmentation in the next section.

Table 2: A comparison of results for augmented (with suffix -A) vs. un-augmented SVD based positional encodings. The presented models have the same specification (in terms of  $L$ ,  $d_h$  and  $d_e$ ) as in Table 1. Also, the names and the suffixes bear the same meaning as in Table 1.

Model	PATTERN		CLUSTER		MNIST	
	Test Acc. $\pm$ s.d.	Train Acc. $\pm$ s.d.	Test Acc. $\pm$ s.d.	Train Acc. $\pm$ s.d.	Test Acc. $\pm$ s.d.	Train Acc. $\pm$ s.d.
EGT-G-SPE	<b>86.730 <math>\pm</math> 0.036</b>	86.804 $\pm$ 0.035	<b>77.909 <math>\pm</math> 0.245</b>	80.730 $\pm$ 0.491	96.675 $\pm$ 0.314	99.641 $\pm$ 0.161
EGT-G-SPE-A	85.624 $\pm$ 0.642	85.604 $\pm$ 0.616	77.626 $\pm$ 0.520	80.165 $\pm$ 1.180	<b>97.573 <math>\pm</math> 0.068</b>	99.550 $\pm$ 0.079

Model	CIFAR10		TSP		ZINC	
	Test Acc. $\pm$ s.d.	Train Acc. $\pm$ s.d.	Test Acc. $\pm$ s.d.	Train Acc. $\pm$ s.d.	Test Acc. $\pm$ s.d.	Train Acc. $\pm$ s.d.
EGT-G-SPE	60.720 $\pm$ 0.883	69.724 $\pm$ 2.089	<b>0.844 <math>\pm</math> 0.001</b>	0.848 $\pm$ 0.002	0.520 $\pm$ 0.008	0.309 $\pm$ 0.018
EGT-G-SPE-A	<b>63.968 <math>\pm</math> 1.252</b>	72.774 $\pm$ 2.751	0.844 $\pm$ 0.002	0.849 $\pm$ 0.003	<b>0.223 <math>\pm</math> 0.007</b>	0.042 $\pm$ 0.007

## 4.2 Ablation Study

To analyze the necessity of augmentation of the SVD based positional encodings by random flipping of the signs of the singular vectors we produced results for both the augmented and un-augmented cases. These results are presented in Table 2. We see that this form of augmentation leads to an improvement in results for the MNIST, CIFAR10 and ZINC datasets. From Table 1, we see that these datasets show a high level of overfitting. Thus, it appears that the need for augmentation arises from the moderate sizes of these datasets and this necessity could be alleviated for larger datasets. To verify this, we conduct the same set of experiments on the larger ZINC-FULL dataset, containing approximately 220K molecules and compare the results with the smaller ZINC dataset (containing 12K molecules). This comparison is presented in Table 4 (see EGT-G-SPE and EGT-G-SPE-A). We see that even though it is crucial to augment the SVD based positional encodings on the smaller dataset to get a good result, this form of augmentation does not lead to an improvement of results on the bigger dataset.

Our architecture is based upon two important ideas - global self-attention based aggregation and residual edge channels. To analyze the importance of these two features, we experiment with different (ablated) variants of our architecture detailed next (results are shown in Table 3).

**Basic Transformer:** First, we experiment with the basic transformer architecture which has no edge channels. This architecture only has residual channels for the nodes. The edge embeddings do not participate in the aggregation process in any way, so the edge features are not used while forming node embeddings. The structural information, i.e., the information about the edges can only be provided in the form of positional encodings. Details about this architecture are presented in subsection 2.2. In subsection 2.4 we showed that SVD based positional encodings can serve to provide enough information to the nodes to approximately reconstruct their connectivity, i.e., the adjacency matrix. Note that, since the adjacency matrix only contains 0/1 values, in practice it

Table 3: Comparison of results for different variants of the EGT architecture with the baseline results for other GNNs. Transformer denotes the basic transformer architecture. It does not take edge features as input, except for the TSP dataset, where the edge features are directly used along with pairwise output node embeddings for edge classification. Structural information is only fed to the Transformer as SVD based positional encodings. The suffix -SPE-16 denotes that rank  $r = 16$  approximation is used to produce the positional encodings. Whereas, the suffix -SPE-FULL denotes that rank  $r = N$  decomposition was used (i.e., a full-rank decomposition). EGT-Simple uses a simplified edge augmentation scheme instead of edge channels. For EGT-simple,  $d_h$  denotes the dimensionality of the edge embeddings rather than the edge channels. EGT-Constrained constrains the aggregation process and the edge channels to a convolutional pattern, within 1-hop neighbors of each node. Other names and suffixes bear the same meaning as in Table 1. Recall that for MAE lower is better.

Model	PATTERN						CLUSTER					
	$L$	#Param	$d_h$	$d_e$	Test Acc. $\pm$ s.d.	Train Acc. $\pm$ s.d.	$L$	#Param	$d_h$	$d_e$	Test Acc. $\pm$ s.d.	Train Acc. $\pm$ s.d.
GAT	16	526990	-	-	78.271 $\pm$ 0.186	90.212 $\pm$ 0.476	16	527874	-	-	70.587 $\pm$ 0.447	61.618 $\pm$ 0.536
GT	10	522742	-	-	83.949 $\pm$ 0.303	83.864 $\pm$ 0.489	10	523146	-	-	72.139 $\pm$ 0.405	85.857 $\pm$ 0.555
GT-EPE-A	10	522982	-	-	84.808 $\pm$ 0.068	86.559 $\pm$ 0.116	10	524026	-	-	73.169 $\pm$ 0.622	86.585 $\pm$ 0.905
GatedGCN	16	502223	-	-	85.568 $\pm$ 0.088	86.007 $\pm$ 0.123	16	502615	-	-	73.840 $\pm$ 0.326	87.880 $\pm$ 0.908
GatedGCN-EPE-A	16	502457	-	-	86.508 $\pm$ 0.085	86.801 $\pm$ 0.133	16	504253	-	-	76.082 $\pm$ 0.196	88.919 $\pm$ 0.720
EGT-G	16	546674	64	8	<b>86.825 <math>\pm</math> 0.032</b>	86.792 $\pm$ 0.044	16	546998	64	8	77.080 $\pm$ 0.361	80.264 $\pm$ 1.251
EGT-G-SPE	16	547762	64	8	86.729 $\pm$ 0.036	86.804 $\pm$ 0.035	16	548086	64	8	<b>77.626 <math>\pm</math> 0.520</b>	80.165 $\pm$ 1.180
Transformer	16	538578	64	-	50.818 $\pm$ 0.067	50.757 $\pm$ 0.037	16	538902	64	-	20.959 $\pm$ 0.063	20.955 $\pm$ 0.034
Transformer-SPE-16	16	540690	64	-	84.844 $\pm$ 0.067	85.338 $\pm$ 0.046	16	541014	64	-	68.313 $\pm$ 0.288	72.076 $\pm$ 0.831
Transformer-SPE-FULL	16	564242	64	-	83.982 $\pm$ 0.021	85.041 $\pm$ 0.309	16	564566	64	-	66.868 $\pm$ 0.285	72.023 $\pm$ 0.559
EGT-Simple-G	16	540898	64	8	86.794 $\pm$ 0.020	86.705 $\pm$ 0.031	16	541222	64	8	76.989 $\pm$ 0.102	80.327 $\pm$ 0.436
EGT-Simple-G-SPE	16	541986	64	8	86.746 $\pm$ 0.055	86.844 $\pm$ 0.031	16	542310	64	8	76.858 $\pm$ 0.218	79.938 $\pm$ 0.524
EGT-Constrained-G	16	546674	64	8	84.267 $\pm$ 0.555	84.261 $\pm$ 0.509	16	546998	64	8	74.532 $\pm$ 0.280	79.324 $\pm$ 1.143
EGT-Constrained-G-EPE-A	16	546674	64	8	84.342 $\pm$ 1.241	84.267 $\pm$ 1.240	16	546998	64	8	75.706 $\pm$ 1.132	79.576 $\pm$ 0.799
EGT-Constrained-G-SPE	16	547762	64	8	86.629 $\pm$ 0.041	86.807 $\pm$ 0.034	16	548086	64	8	76.701 $\pm$ 0.257	79.528 $\pm$ 1.349

Model	MNIST						CIFAR10					
	$L$	#Param	$d_h$	$d_e$	Test Acc. $\pm$ s.d.	Train Acc. $\pm$ s.d.	$L$	#Param	$d_h$	$d_e$	Test Acc. $\pm$ s.d.	Train Acc. $\pm$ s.d.
GAT	4	110400	-	-	95.535 $\pm$ 0.205	99.994 $\pm$ 0.008	4	110704	-	-	64.223 $\pm$ 0.455	89.114 $\pm$ 0.536
GatedGCN	4	104217	-	-	97.340 $\pm$ 0.143	100.000 $\pm$ 0.000	4	104357	-	-	<b>67.312 <math>\pm</math> 0.311</b>	87.880 $\pm$ 0.908
EGT-G	4	138826	64	8	97.615 $\pm$ 0.050	99.346 $\pm$ 0.211	4	138945	64	8	63.260 $\pm$ 0.735	71.878 $\pm$ 1.363
EGT-G-SPE-A	4	139914	64	8	97.573 $\pm$ 0.068	99.550 $\pm$ 0.079	4	140042	64	8	63.968 $\pm$ 1.252	72.774 $\pm$ 2.751
Transformer	4	137050	64	-	97.680 $\pm$ 0.406	99.271 $\pm$ 0.350	4	137178	64	-	58.350 $\pm$ 0.514	66.186 $\pm$ 1.461
Transformer-SPE-16	4	139162	64	-	96.988 $\pm$ 0.356	99.124 $\pm$ 0.358	4	139290	64	-	53.922 $\pm$ 3.666	63.267 $\pm$ 5.191
Transformer-SPE-FULL	4	149914	64	-	96.380 $\pm$ 0.394	99.376 $\pm$ 0.238	4	156442	64	-	49.833 $\pm$ 1.010	60.791 $\pm$ 1.989
EGT-Simple-G	4	137658	64	8	<b>97.940 <math>\pm</math> 0.192</b>	99.433 $\pm$ 0.168	4	137786	64	8	62.840 $\pm$ 0.648	71.441 $\pm$ 0.765
EGT-Simple-G-SPE-A	4	138746	64	8	97.487 $\pm$ 0.438	98.954 $\pm$ 0.624	4	138874	64	8	63.260 $\pm$ 0.569	71.404 $\pm$ 1.730
EGT-Constrained-G	4	138826	64	8	96.753 $\pm$ 0.297	99.587 $\pm$ 0.554	4	138954	64	8	63.165 $\pm$ 0.139	70.843 $\pm$ 0.177
EGT-Constrained-G-SPE-A	4	139914	64	8	96.823 $\pm$ 0.204	99.359 $\pm$ 0.462	4	140042	64	8	65.192 $\pm$ 0.475	75.393 $\pm$ 1.470

Model	TSP						ZINC					
	$L$	#Param	$d_h$	$d_e$	Test F1 $\pm$ s.d.	Train F1 $\pm$ s.d.	$L$	#Param	$d_h$	$d_e$	Test MAE $\pm$ s.d.	Train MAE $\pm$ s.d.
GAT	4	96182	-	-	0.671 $\pm$ 0.002	0.673 $\pm$ 0.002	16	531345	-	-	0.384 $\pm$ 0.007	0.067 $\pm$ 0.004
GT							10	588353	-	-	0.264 $\pm$ 0.008	0.048 $\pm$ 0.006
GT-EPE-A							10	588939	-	-	0.226 $\pm$ 0.014	0.059 $\pm$ 0.011
GatedGCN	16	500770	-	-	0.838 $\pm$ 0.002	0.850 $\pm$ 0.001	16	504309	-	-	0.282 $\pm$ 0.015	0.074 $\pm$ 0.016
GatedGCN-EPE-A							16	505011	-	-	0.214 $\pm$ 0.013	0.067 $\pm$ 0.019
EGT-G	16	524226	64	8	<b>0.845 <math>\pm</math> 0.001</b>	0.850 $\pm$ 0.002	10	506977	64	64	0.302 $\pm$ 0.023	0.067 $\pm$ 0.017
EGT-G-SPE-A	16	525314	64	8	0.844 $\pm$ 0.002	0.849 $\pm$ 0.003	10	508065	64	64	0.223 $\pm$ 0.007	0.042 $\pm$ 0.007
							16	532425	56	40	0.227 $\pm$ 0.007	0.044 $\pm$ 0.011
Transformer	16	540850	64	-	0.610 $\pm$ 0.032	0.610 $\pm$ 0.032	16	540161	64	-	0.694 $\pm$ 0.003	0.623 $\pm$ 0.004
Transformer-SPE-16	16	542962	64	-	0.792 $\pm$ 0.007	0.795 $\pm$ 0.007	16	542273	64	-	0.692 $\pm$ 0.010	0.597 $\pm$ 0.023
Transformer-SPE-FULL	16	604914	64	-	0.773 $\pm$ 0.010	0.776 $\pm$ 0.011	16	545345	64	-	0.693 $\pm$ 0.015	0.601 $\pm$ 0.041
EGT-Simple-G	16	543154	64	8	0.818 $\pm$ 0.002	0.821 $\pm$ 0.002	10	528857	80	8	0.383 $\pm$ 0.025	0.208 $\pm$ 0.046
EGT-Simple-G-SPE-A	16	544242	64	8	0.819 $\pm$ 0.002	0.823 $\pm$ 0.003	10	530217	80	8	0.266 $\pm$ 0.034	0.067 $\pm$ 0.026
EGT-Constrained-G	16	524226	64	8	<b>0.846 <math>\pm</math> 0.001</b>	0.851 $\pm$ 0.003	10	506977	64	64	0.232 $\pm$ 0.010	0.051 $\pm$ 0.014
EGT-Constrained-G-EPE-A							10	506977	64	64	0.184 $\pm$ 0.006	0.058 $\pm$ 0.020
EGT-Constrained-G-SPE-A	16	525314	64	8	<b>0.846 <math>\pm</math> 0.001</b>	0.852 $\pm$ 0.001	10	508065	64	64	0.189 $\pm$ 0.011	0.071 $\pm$ 0.028
							16	532425	56	40	<b>0.174 <math>\pm</math> 0.004</b>	0.048 $\pm$ 0.024

can be reconstructed from a lower rank approximation via SVD. We experimented with two forms of positional encodings – for  $r = 16$  and  $r = N$  in equation (22).  $r = N$  denotes a full rank approximation where the adjacency matrix can be completely reconstructed from the positional encodings. Since edge embeddings are absent in the transformer architecture edge classification is performed from pairwise node embeddings and input edge features.

Table 4: A comparison of results between the smaller ZINC (12K molecular graphs) and the larger ZINC-FULL ( 220K molecular graphs) datasets. The names and the suffixes bear the same meaning as in Table 1 and Table 3.

Model	$L$	#Param	$d_h$	$d_e$	ZINC		ZINC-FULL	
					Test Acc. $\pm$ s.d.	Train Acc. $\pm$ s.d.	Test Acc. $\pm$ s.d.	Train Acc. $\pm$ s.d.
EGT-G	10	506977	64	64	$0.302 \pm 0.023$	$0.067 \pm 0.017$	$0.051 \pm 0.002$	$0.031 \pm 0.004$
EGT-G-SPE	10	508065	64	64	$0.520 \pm 0.008$	$0.309 \pm 0.018$	<b><math>0.042 \pm 0.005</math></b>	$0.023 \pm 0.004$
EGT-G-SPE-A	10	508065	64	64	$0.223 \pm 0.007$	$0.042 \pm 0.007$	$0.046 \pm 0.001$	$0.027 \pm 0.002$
Transformer	16	540161	64	-	$0.694 \pm 0.003$	$0.623 \pm 0.004$	$0.632 \pm 0.002$	$0.617 \pm 0.004$
Transformer-SPE-16	16	542273	64	-	$0.692 \pm 0.010$	$0.597 \pm 0.023$	$0.138 \pm 0.014$	$0.078 \pm 0.012$
Transformer-SPE-FULL	16	545345	64	-	$0.693 \pm 0.015$	$0.601 \pm 0.041$	$0.130 \pm 0.016$	$0.073 \pm 0.014$
EGT-Simple-G	10	528857	80	8	$0.383 \pm 0.025$	$0.208 \pm 0.046$	$0.056 \pm 0.001$	$0.033 \pm 0.006$
EGT-Simple-G-SPE	10	530217	80	8	$0.387 \pm 0.013$	$0.204 \pm 0.052$	$0.049 \pm 0.002$	$0.025 \pm 0.004$
EGT-Simple-G-SPE-A	10	530217	80	8	$0.266 \pm 0.034$	$0.067 \pm 0.026$	$0.048 \pm 0.003$	$0.022 \pm 0.004$
EGT-Constrained-G	10	506977	64	64	$0.232 \pm 0.010$	$0.051 \pm 0.014$	$0.063 \pm 0.004$	$0.027 \pm 0.002$
EGT-Constrained-G-SPE	10	508065	64	64	$0.465 \pm 0.021$	$0.206 \pm 0.088$	$0.051 \pm 0.003$	$0.028 \pm 0.002$
EGT-Constrained-G-SPE-A	10	508065	64	64	<b><math>0.184 \pm 0.006</math></b>	$0.058 \pm 0.020$	$0.048 \pm 0.002$	$0.027 \pm 0.003$

The results are presented in Table 3. We notice that the results for the basic transformer are either comparable to or worse than EGT. The inclusion of SVD based positional encodings results in the greatest improvement for PATTERN, CLUSTER and TSP datasets since the node features in this dataset contain no information about the edges and the targeted task is either impossible or difficult to perform without this information. On the other hand, positional encodings are less important for MNIST and CIFAR10 for which indirect information about the edges is present in form of coordinates of the superpixels within the node features. It seems that the positional encodings do not improve the results on the ZINC dataset. Also, a full-rank decomposition does not improve the results. However, both of these are results of overfitting and from the results on the ZINC-FULL dataset in Table 4, we can confirm that given enough data positional encodings do indeed improve the results significantly, and a full-rank decomposition can help improve the results, albeit moderately.

**EGT-Simple:** Next, we experiment with a variant of EGT whereby we use global self-attention, but instead of having dedicated residual channels for edges, we directly use the edge embeddings (formed from adjacency matrix and edge features) in the aggregation process. Equation (12) and (13) are modified as:

$$\hat{w}_{ij}^{k,\ell} = \max \left( \mu, \min \left( \nu, \frac{(\mathbf{Q}^{k,\ell} \hat{h}_i^\ell)^T (\mathbf{K}^{k,\ell} \hat{h}_j^\ell)}{\sqrt{d_k}} \right) \right) + E^{k,\ell} e_{ij}^0 \quad (25)$$

$$w_{ij}^{k,\ell} = \text{softmax}_j \left( \hat{w}_{ij}^{k,\ell} \right) \sigma(G^{k,\ell} e_{ij}^0) \quad (26)$$

Notice that, input edge embeddings  $e_{ij}^0$  are directly used. Also, the absence of an edge channel means that the edge embeddings  $e_{ij}$  are not updated from layer to layer. So, edge classification is performed in a similar manner to the basic transformer. We denote this variant as EGT-Simple since it is architecturally simpler than EGT. It is also similar to the Graph Transformer proposed by Li et al. [14]. This architecture also is slightly less expensive in terms of computation and memory, although it scales quadratically with the number of nodes. From the results in Table 3 and 4, we see that this architecture can come very close to EGT in terms of performance. However, performance is especially subpar compared to EGT when the targeted task is related to edges (e.g., edge classification on the TSP dataset). This is due to the lack of dedicated edge channels which can update pairwise information from layer to layer.

**EGT-Constrained:** Finally, we compare global self-attention to convolutional local self-attention based aggregation. To this end, we limit the self-attention process to the 1-hop neighborhood of each node. Also, we only keep track of the edge embeddings  $e_{ij}$  in the edge channels if there is an edge from node  $i$  to node  $j$  or  $i = j$  (self-loop). So, pairwise information corresponding to only the existing edges is updated by the edge channels. This architecture can be derived by taking the softmax in equation (13) over  $j \in \mathcal{N}(i) \cup \{i\}$  and limiting the aggregation process in equation (16) to neighbors as:

$$\hat{h}_i^\ell = h_i^{\ell-1} + \mathbf{O}_h^\ell \parallel \sum_{k=1}^H \sum_{j \in \mathcal{N}(i) \cup \{i\}} w_{ij}^{k,\ell} \mathbf{V}^{k,\ell} \hat{h}_i^\ell \quad (27)$$

Since this architecture is constrained to the existing edges we denote this as EGT-Constrained. It has the advantage that depending on the sparsity of the graph, it can have sub-quadratic computational and memory costs. However, it can be difficult to do sparse aggregation in parallel on the GPU. Instead of sparse operations, we used masked attention to implement this architecture for faster training on datasets containing smaller graphs because we can take advantage of highly parallel tensor operations. Architecturally, this variant is very similar to GT [10]. From the results in Table 3 and 4 we see that EGT-Constrained consistently benefits from inclusion of positional encodings. This verifies our statement that positional encodings are more important when we perform local aggregation because they serve to provide global information to the nodes. Also, we see that SVD based positional encodings perform equivalently or better than Laplacian eigenvectors even when we follow a convolutional aggregation pattern. Further, the results are better than GT, which uses a very similar architecture. This architecture achieves results that are equivalent or slightly below EGT on most datasets except CIFAR10 and ZINC. The results on these two datasets are better than that of EGT because EGT-Constrained uses the convolutional aggregation pattern as an inductive bias whereas EGT learns the best aggregation pattern from data which leads to overfitting. This is further evidenced by the fact that on the bigger ZINC-FULL dataset EGT-Constrained loses its advantage over EGT and performs slightly worse (Table 4). This result suggests that given enough data, global self-attention based aggregation can outperform local self-attention based convolutional aggregation.

## 5 Conclusion

We proposed a simple extension – edge channels – to the transformer framework, which makes it directly applicable to graphs. We preserve the key idea behind the original transformer architecture – global attention – while making it powerful enough to take structural information as input and also to process it and output new structural information such as new links and edge labels. One of our key findings has been that the incorporation of the convolutional aggregation pattern is not an essential inductive bias for GNNs and instead the model can directly learn to make the best use of structural information. We established this claim by presenting experimental results on 6 benchmark datasets and comparing our architecture against well-known convolutional GNNs. Also, we generalized the Laplacian eigenvectors based positional encoding scheme to form a novel SVD-based positional encoding scheme which is shown to improve the performance of our architecture on several tasks.

We experimented with our model in an inductive and supervised setting only. But it can be used in transductive and/or semi-supervised settings as well. However, we could not perform those tests due to constraints in terms of computational cost and dataset size. Also, our model can be used to learn representations in an unsupervised manner similar to Graph-BERT [3]. Our framework has the added benefit of direct input of structural information and masking of edges which can help in this setting. We aim to perform more experiments to verify the effectiveness of our network for unsupervised learning in future work.

Our model uses global self-attention just like the original transformer architecture, which incurs a quadratic computational and memory cost. However, recently there has been an increasing number of works that aim at reducing the complexity of global self-attention to a linear cost by a factorization of the self-attention matrix [40, 41, 42]. The edge channels which we conceived to have a quadratic number of non-zero elements, can be constrained to some sparsity pattern based on hops, or some other form of intimacy metric (e.g., page rank). By combining these two optimizations of the architecture the overall computational and memory cost could be reduced to sub-quadratic or even linear. This would allow for our architecture to be directly applicable to bigger graphs with a large number of nodes. We plan on exploring this in future work.

## References

- [1] Ashish Vaswani et al. “Attention is all you need”. In: *Advances in neural information processing systems*. 2017, pp. 5998–6008.
- [2] Mark Chen et al. “Generative Pretraining from Pixels”. In: *International Conference on Machine Learning*. PMLR, 2020, pp. 1691–1703.
- [3] Jiawei Zhang et al. *Graph-Bert: Only Attention Is Needed for Learning Graph Representations*. 2020. arXiv: 2001.05140.

- [4] Vijay Prakash Dwivedi et al. *Benchmarking Graph Neural Networks*. 2020. arXiv: 2003.00982.
- [5] Jean-Baptiste Cordonnier, Andreas Loukas, and Martin Jaggi. *On the Relationship between Self-Attention and Convolutional Layers*. 2019. arXiv: 1911.03584.
- [6] Prajit Ramachandran et al. *Stand-Alone Self-Attention in Vision Models*. 2019. arXiv: 1906.05909.
- [7] Omri Puny, Heli Ben-Hamu, and Yaron Lipman. *Global Attention Improves Graph Networks Generalization*. 2020. arXiv: 2006.07846.
- [8] Chen Wang and Chengyuan Deng. “On the Global Self-Attention Mechanism for Graph Convolutional Networks”. In: *2020 25th International Conference on Pattern Recognition (ICPR)*. IEEE, 2021, pp. 8531–8538.
- [9] Petar Veličković et al. “Graph attention networks”. In: *arXiv preprint arXiv:1710.10903* (2017).
- [10] Vijay Prakash Dwivedi and Xavier Bresson. *A Generalization of Transformer Networks to Graphs*. 2020. arXiv: 2012.09699.
- [11] Thomas N Kipf and Max Welling. “Semi-supervised classification with graph convolutional networks”. In: *arXiv preprint arXiv:1609.02907* (2016).
- [12] William L. Hamilton, Rex Ying, and Jure Leskovec. *Inductive Representation Learning on Large Graphs*. 2017. arXiv: 1706.02216.
- [13] Keyulu Xu et al. *How Powerful Are Graph Neural Networks?* 2018. arXiv: 1810.00826.
- [14] Yuan Li et al. “Graph Transformer”. In: (2018).
- [15] Dai Quoc Nguyen, Tu Dinh Nguyen, and Dinh Phung. *Universal Self-Attention Network for Graph Classification*. 2019. arXiv: 1909.11855.
- [16] Ziniu Hu et al. “Heterogeneous Graph Transformer”. In: *Proceedings of The Web Conference 2020*. 2020, pp. 2704–2710.
- [17] Seongjun Yun et al. *Graph Transformer Networks*. 2019. arXiv: 1911.06455.
- [18] Ryan Murphy et al. “Relational pooling for graph representations”. In: *International Conference on Machine Learning*. PMLR. 2019, pp. 4663–4673.
- [19] Balasubramaniam Srinivasan and Bruno Ribeiro. “On the equivalence between positional node embeddings and structural graph representations”. In: *arXiv preprint arXiv:1910.00452* (2019).
- [20] Sergey Ioffe and Christian Szegedy. “Batch Normalization: Accelerating Deep Network Training by Reducing Internal Covariate Shift”. In: *International Conference on Machine Learning*. PMLR, 2015, pp. 448–456.
- [21] Jimmy Lei Ba, Jamie Ryan Kiros, and Geoffrey E. Hinton. *Layer Normalization*. 2016. arXiv: 1607.06450.
- [22] Kaiming He et al. “Deep Residual Learning for Image Recognition”. In: *Proceedings of the IEEE Conference on Computer Vision and Pattern Recognition*. 2016, pp. 770–778.
- [23] Ruibin Xiong et al. “On Layer Normalization in the Transformer Architecture”. In: *International Conference on Machine Learning*. PMLR, 2020, pp. 10524–10533.
- [24] Djork-Arné Clevert, Thomas Unterthiner, and Sepp Hochreiter. *Fast and Accurate Deep Network Learning by Exponential Linear Units (Elus)*. 2015. arXiv: 1511.07289.
- [25] Jiaxuan You, Rex Ying, and Jure Leskovec. “Position-Aware Graph Neural Networks”. In: *International Conference on Machine Learning*. PMLR, 2019, pp. 7134–7143.
- [26] Mikhail Belkin and Partha Niyogi. “Laplacian Eigenmaps and Spectral Techniques for Embedding and Clustering.” In: *Nips*. Vol. 14. 14. 2001, pp. 585–591.
- [27] Muhan Zhang et al. *Revisiting Graph Neural Networks for Link Prediction*. 2020. arXiv: 2010.16103.
- [28] Andrew Kachites McCallum et al. “Automating the construction of internet portals with machine learning”. In: *Information Retrieval 3.2* (2000), pp. 127–163.
- [29] Lise Getoor. “Link-based classification”. In: *Advanced methods for knowledge discovery from complex data*. Springer, 2005, pp. 189–207.
- [30] Christopher Morris et al. “Tudataset: A collection of benchmark datasets for learning with graphs”. In: *arXiv preprint arXiv:2007.08663* (2020).
- [31] Emmanuel Abbe. “Community Detection and Stochastic Block Models: Recent Developments”. In: *The Journal of Machine Learning Research* 18.1 (2017), pp. 6446–6531.



- [32] Radhakrishna Achanta et al. “SLIC Superpixels Compared to State-of-the-Art Superpixel Methods”. In: *IEEE transactions on pattern analysis and machine intelligence* 34.11 (2012), pp. 2274–2282.
- [33] Yann LeCun et al. “Gradient-Based Learning Applied to Document Recognition”. In: *Proceedings of the IEEE* 86.11 (1998), pp. 2278–2324.
- [34] Alex Krizhevsky and Geoffrey Hinton. “Learning Multiple Layers of Features from Tiny Images”. In: (2009).
- [35] John J. Irwin et al. “ZINC: A Free Tool to Discover Chemistry for Biology”. In: *Journal of chemical information and modeling* 52.7 (2012), pp. 1757–1768.
- [36] Diederik P. Kingma and Jimmy Ba. *Adam: A Method for Stochastic Optimization*. 2014. arXiv: 1412.6980.
- [37] Martín Abadi et al. “Tensorflow: A System for Large-Scale Machine Learning”. In: *12th USENIX Symposium on Operating Systems Design and Implementation (OSDI 16)*. 2016, pp. 265–283.
- [38] William L Hamilton, Rex Ying, and Jure Leskovec. “Representation learning on graphs: Methods and applications”. In: *arXiv preprint arXiv:1709.05584* (2017).
- [39] Xavier Bresson and Thomas Laurent. *Residual Gated Graph Convnets*. 2017. arXiv: 1711.07553.
- [40] Krzysztof Choromanski et al. “Rethinking attention with performers”. In: *arXiv preprint arXiv:2009.14794* (2020).
- [41] Angelos Katharopoulos et al. “Transformers Are Rnns: Fast Autoregressive Transformers with Linear Attention”. In: *International Conference on Machine Learning*. PMLR, 2020, pp. 5156–5165.
- [42] Imanol Schlag, Kazuki Irie, and Jürgen Schmidhuber. *Linear Transformers Are Secretly Fast Weight Memory Systems*. 2021. arXiv: 2102.11174.